
**Journal of Macromolecular Science, Part B**
Publication details, including instructions for authors and subscription information:
http://www.informaworld.com/smpp/title~content=t713375300

# Toward a Physical Definition of Entanglements

José A. Martins[ab]
[a] Departamento de Engenharia de Polímeros, Universidade do Minho, Campus de Azurém Guimarães, Portugal [b] CICECO, Universidade de Aveiro, Aveiro, Portugal

Online publication date: 03 March 2011

**To cite this Article** Martins, José A.(2011) 'Toward a Physical Definition of Entanglements', Journal of Macromolecular Science, Part B, 50: 4, 769 — 794
**To link to this Article: DOI:** 10.1080/00222341003785151
**URL:** http://dx.doi.org/10.1080/00222341003785151

*Journal of Macromolecular Science®, Part B: Physics*, 50:769–794, 2011

ISSN: 0022-2348 print / 1525-609X online
DOI: 10.1080/00222341003785151

Taylor & Francis
Taylor & Francis Group

# Toward a Physical Definition of Entanglements

JOSÉ A. MARTINS[1,2]

[1]Departamento de Engenharia de Polímeros, Universidade do Minho, Campus de Azurém Guimarães, Portugal
[2]CICECO, Universidade de Aveiro, Aveiro, Portugal

*To examine the role of chain entanglements on polymer melt properties, the interaction potential energy between a loop and chain at its center is evaluated. The interaction potential energy between binary contacts of two adjacent Kuhn monomers is also evaluated. The elasticity in polymer melts and the evaluation of the different contributions to flow activation energy of linear polymer chains are used to demonstrate that chain loops, or any other binary interactions between polymer chain segments, cannot justify the properties assigned to entanglements. These properties may be understood if interactions between several parallel chain segments are considered instead, which implies the assumption of the existence of short-range local ordered regions in polymer melts. Their existence is demonstrated from abundant literature experiments, molecular dynamics simulation results, and also from a detailed discussion on the interaction potential energy values. Because more than 80% of the conformational states in one chain are random sequences of chain segments, the remaining states being in short-range ordered regions, we conclude that the random coil model is not an exact model for the morphology of polymer melts, but it is still a very good description of chain conformations in the molten state.*

**Keywords** entanglements, flow activation energy, intermolecular interactions, polymer melts.



## Introduction

The importance of intermolecular interactions between polymer chains has been recognized by a series of research works published since the word entanglement in polymer science was introduced by Busse in 1932.[1] The excerpt below illustrates their relevance. "As a result of the flexibility of polymer chains, their dynamic behavior is quite complicated. In polymer melts, and also in concentrated polymer solutions, the situation is aggravated by the fact that each chain is interacting with many other chains. The effect of these intermolecular interactions is best revealed by the peculiar flow behavior of these materials: they are very viscous and have surprising elastic properties. In uncrosslinked polymers, these elastic properties manifest themselves temporarily, but still sometimes on very long time scales (hours). So, despite the fact that they are not crosslinked (as in a rubber), dense polymer systems act temporarily as rubber-like networks. The cause of this, of course, is the fact that the chains are intertwined and can not penetrate through each other: they are 'entangled.'

Received 4 February 2010; accepted 5 March 2010.
Address correspondence to José A. Martins, Departamento de Engenharia de Polímeros, Universidade do Minho, Campus de Azurém 4800-058 Guimarães, Portugal. E-mail: jamartins@dep.uminho.pt

These entanglements survive for some non-negligible time. Another interesting observation is that the magnitude of the elastic effect is rather independent of chain length, but it occurs only when the chains are longer than a certain threshold."[2]

It is considered in a recent work[3] that the *strong interaction* due to entanglements, responsible for the effects described above, does not result necessarily from the looping of one molecule around another, "*but more simply from the fact that the displacement of one molecule due to Brownian motion is highly constrained laterally by the other molecules*" (page 17), and that this constraining results from the impossibility of polymer chains to pass through each other (the chain uncrossability). Later on, in this reference (page 203), it is concluded that "*a precise definition of an entanglement has not been generally agreed upon, . . . , an entanglement is a topological interaction between one polymer molecule and its neighbors that greatly impedes its motion.*" These sentences deserve a careful critical analysis.

These authors,[3] and many others, consider that entanglements are "strong topological interactions." In physics, any interaction is described with a force, which is related to a potential, and there are only four fundamental forces in nature: gravitic, electromagnetic, weak, and strong; *topological interaction is not among them*. By saying that entanglement effects do not result necessarily from chain looping, it is not concluded clearly what is the role of chain loops in entanglement effects. Another surprising and contradictory statement is the assignment of entanglement effects to the constraining effect of neighboring chains on the motion of one chain segment—the chain uncrossability. Physically, chain uncrossability results from hard-core repulsive interactions, and repulsive potentials cannot explain elastic effects such as those responsible for plateau modulus in entangled polymer melts or the increase in the zero-shear rate viscosity with exponent of 3.4 in the weight-average molecular weight.

It is known that thermal agitation of molecules due to their Brownian motion induces electromagnetic fluctuations and that these fluctuations arise also in electrically neutral bodies as the result of quantum mechanical uncertainties in the position and momenta of their particles.[4,5] These electromagnetic fluctuations yield the van der Waals interactions, which are far more powerful in condensed phases than in gases. Therefore, the constraining in the Brownian motion of one molecule by other molecules implies that van der Waals interactions exist between them. So far, values for the van der Waals interaction energy between chain segments in the molten state are nonexistent in the literature we have searched. It seems clear, however, that the above mentioned strong interaction due to entanglements must be higher than the melt thermal energy.

One may envisage, then, different geometrical arrangements between chain segments accounting for the chain uncrossability and evaluate quantitatively the associated attractive interaction potentials. Since it is considered that, during chain intertwining, polymer chains cannot pass through each other, we evaluate below the interaction potential energy associated to the intertwining of polymer chains. To cope with this problem, the interaction between a chain and a loop is considered as an adequate geometrical representation of the chain intertwining. To explain the elasticity in polymer melts, this interaction potential energy must have a non-negligible value, more specifically, it must be higher than the thermal energy of the melt.

Because another type of interaction that prevents chains to cross each other is that involving two Kuhn monomers, of the same or of different chains, aligned in parallel and separated from each other by a distance equal to the nearest neighbor intermolecular packing distance, this interaction potential energy is also evaluated. Another interaction that has still to be considered is that involving, not only two, but several adjacent and parallel

Kuhn monomers. Of course, in this case one has to consider the existence of short-range local ordered regions in polymer melts.

It is unclear, now, which of these three different interactions, all accounting for chain uncrossability, has higher magnitude. It is their relative magnitude that will determine which one of them has a leading role on general melt properties.

The structure of this work is the following: in the "Interaction Potential Energy between Two Parallel Chain Segments" section the main assumptions made in the derivation of an expression for evaluating the interaction potential energy between two parallel chain segments are discussed and it is shown how to extend the evaluation for interactions involving one chain segment and a set of other aligned neighboring chain segments; in the next section an expression is derived for evaluating the interaction potential energy between a loop and a chain at its center; in the next section the validity of results obtained for these two evaluations is discussed; in the next section the different contributions to the flow energy barrier are discriminated, their value evaluated from literature results, and a physical meaning is assigned to the flow energy of polymer melts in the high-temperature flow region. It will be shown that, for linear polymer chains, there are mainly two contributions. One is an intramolecular contribution, and it is related to the energy barriers for local and correlated conformational transitions. The other is an intermolecular contribution, and it will be shown that it cannot be explained by considering the interaction potential energy between a loop and a chain (or even several chain loops in a number equal to that of entanglements), or still any other binary interaction between chain segments. Based on this result, a new model for the polymer melt morphology is presented and its conformity with the random coil model is discussed.



## Interaction Potential Energy between Two Parallel Chain Segments

Expressions for evaluating the interaction potential energy between two parallel and aligned chain segments were derived in 1962 by Salem.[6] They consider only dipole–dipole interactions and agree with a previous evaluation for the interaction potential energy between two parallel rods with infinite length made by de Rocco and Hoover in 1960.[7]]

The solution to the problem of the interaction potential energy between two parallel chains was solved by assuming that the molecules in the chain are distributed according to a function of position, and that the interaction of pairs of molecules is well represented by a pair potential $W(r_{ij})$, where $r_{ij}$ is the distance separating mer $n_i$ in chain 1 from mer $n_j$ in chain 2 and the attractive contribution of $W(r_{ij})$ is expressed by a London law $W = -C/r^6$, where $C$ is the London constant for the interaction between the two chains. The additivity of interactions is considered, and it is expressed as a double-sum of the pair potential interactions running from $n_i = 1$ to $N$, for all $n_i$ mers of chain 1 with all $n_j$ mers of chain 2, from $n_j = 1$ to $N$ and vice-versa, where $N$ is the number of mers in each chain—see Fig. 1.

The discrete form of the equation derived by Salem for the interaction potential energy between two parallel chains is

$$W_c = -C\left[\frac{N}{D^6} + 2\sum_{x=1}^{N-1}\frac{(N-x)}{(D^2+\lambda^2x^2)^3}\right], \tag{1}$$

where $D$ is the separation distance between two parallel chains, taken from the axis of each chain, $\lambda$ is the separation distance between consecutive mers in the chain, and $\lambda x$ is the

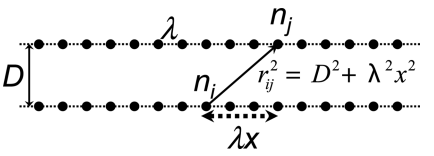


**Figure 1.** Model used to evaluate the interaction potential energy between two parallel chains. Chain 1 has $n_j$ mers and chain 2 has $n_j$ mers. The two chains are separated from each other by a distance $D$. The consecutive mers in any chain are separated by $\lambda$. The distance along the axis of one chain between mer $n_i$ in chain 1 and mer $n_j$ in chain 2 is $\lambda|n_i - n_j|$. The distance between two mers in the two chains is $r_{ij}$, and it is evaluated by application of the Pythagorean theorem.

distance along the chain axis between mers in chains 1 and 2, with $x = |n_i - n_j|$. Derivation of Equation (1) contains three assumptions: the pairwise additivity of interactions, the chain isotropy, and the absence of intrachain van der Waals interactions.

The corresponding continuous version is obtained under the additional assumptions of very long chains and chain separation $D$ much lower than the chain's length $L = N\lambda$. The result is

$$W_c = -3\pi CL/8\lambda^2 D^5. \tag{2}$$

Extension of the above two equations to evaluate the interaction potential energy between a reference chain and a set of other surrounding chains is easily obtained by multiplying the above two equations, (1) and (2), by the number of neighboring chains. For two parallel chains, this number is 1.

The criticisms raised to the application of Salem's equation[8–10] for evaluating the interaction potential energy between two parallel chains were related not to the dependence of $W_c$ on $L/\lambda^2 D^5$, but specifically to the evaluation of the London constant $C$. This specific issue is discussed below in the "Validity of Results Obtained for the Interaction Potential Energy" section. For the moment, it is suffices to state that in the framework of the modern theory of van der Waals interaction, also known as Lifshitz theory, the London constant $C$ is related to the Hamaker constant $A$ by $A = \pi^2 \rho_1 \rho_2 C$, where $\rho_1$ and $\rho_2$ are the number of atoms per unit of volume in chains 1 and 2, respectively.[5]

The main advantage of Lifshitz theory of van der Waals interactions is treating the interacting bodies as continuous media. In this way, the problem of the pairwise additivity, intrinsic to the above equations, is ignored, and the forces between the two bodies are expressed in terms of their dielectric constants and refractive indexes. In this new formulation, Equations (1) and (2) remain the same, the only difference being that, in the framework of Lifhistz theory, the Hamaker constant is expressed by[5]

$$A_{total} = A_{\nu=0} + A_{\nu>0} = \frac{3}{4} k_B T \left(\frac{\varepsilon - \varepsilon_o}{\varepsilon + \varepsilon_o}\right)^2 + \frac{3h\nu_e}{16\sqrt{2}} \cdot \frac{\left(n^2 - n_o^2\right)^2}{\left(n^2 + n_o^2\right)^{3/2}}, \tag{3}$$

where $\varepsilon$ and $\varepsilon_o$ are the static dielectric constants for the polymer and vacuum, $n$ and $n_o$ are the corresponding refractive indexes, $h$ and $k_B$, the Planck and Boltzmann constants, respectively, $T$ the absolute temperature and $\nu_e$ the main electronic absorption frequency in the UV ($\cong 2.4 \times 10^{15}$ Hz). The total Hamaker constant for two identical chains interacting across vacuum contains an entropic zero-frequency contribution ($A_{\nu=0}$), which includes the Keesom and Debye dipolar contributions to the van der Waals interactions, and a dispersion

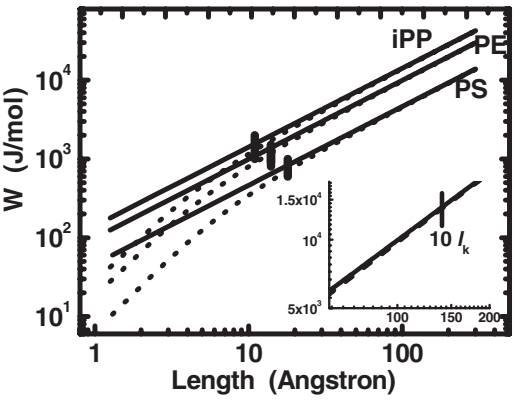


**Figure 2.** Absolute values of the interaction potential energy between parallel chain segments of different polymers evaluated with Equations (1)—dotted line—and (2)—solid line, for segments starting with length λ up to 239xλ , or 300 Å. The short vertical lines indicate the length of one Kuhn monomer for each polymer. Data used in this evaluation are in Table 1 and Table A1. The inset shows the interaction potential energy of polyethylene for chain segments with length around 10 Kuhn monomers.



energy contribution ($A_{\nu>0}$), which includes the London energy contribution.[5] In the above equation retardation effects due to the finite velocity of light were ignored. These effects are important only when the distance of separation between two interacting molecules is large enough for the suppression of the interaction. This issue is also discussed in the "Validity of Results Obtained for the Interaction Potential Energy" section.

Results obtained with Equations (1)—dotted lines—and (2)—solid lines—for the absolute value of the interaction potential energy of several polymers are indicated in Fig. 2. Because we are discussing only attractive interactions, all results and discussion below will be presented in terms of absolute values of the interaction potential energy. Although the results indicated refer to the interaction between two parallel chain segments with the length indicated in the figure, the chain segments need not necessarily be strictly parallel and straight. As shown below, Equations (1) and (2) are also valid when the chain segments run in parallel, but are not necessarily straight. In any case, the square of the distance between any $n_i$th atom of chain 1 and any $n_j$th atom of chain 2 is given by $r^2 = D^2 + \lambda^2(n_i - n_j)^2$.

The data used to evaluate the interaction potential energy are in Table I. Additional relevant information for the polymers considered here is in Table II and the Appendix. Only linear polymer chains are considered here. Because we are interested in evaluating the interaction potential energy in the molten state, the temperature dependent parameters, namely the Hamaker constant and the number density of atoms per unit volume in each chain, were evaluated at 200°C. Also, values for the separation distance between chain segments were obtained from WAXD experimental results for polymer melts and results of molecular dynamics simulations—see the Appendix.

The interaction potential energy of two parallel Kuhn monomers of polypropylene and polyethylene, lengths of 11 Å and 14 Å, respectively, is around 1 kJ mol$^{-1}$. That of two Kuhn monomers of PS, length 18 Å, is around 0.7 kJ mol$^{-1}$. All these values are below the melt thermal energy ($RT \approx 3.9$ kJ mol$^{-1}$ at 200°C, where $R$ is the ideal gas constant). For interactions between two Kuhn monomers, the deviation between the discrete and

**Table 1**

Data used to evaluate the interaction potential energy at $T = 200^{\circ}$C. $V_{vw}$ is the van der Waals volume of the repeated unit, $\rho$ is the number density of molecules in the repeated unit, $A$ is the Hamaker constant, $C$ is the London constant, $\lambda$ is the separation distance between consecutive molecules in the chain at the chain axis, and $D$ is the separation distance between two parallel chain segments (it is also the value of the radius of the loop). The absolute values of the interaction potential energy for a loop and a chain ($W_l$)—Equation (5)—and two parallel chains segments with a length equal to a Kuhn monomer ($W_k$) are indicated. The last row contains two values for $W_k$: the first was evaluated with Equation (2) and the last one with Equation (1)

| | PE | PP | PS |
|---|---|---|---|
| $V_{vw}$ (Å$^3$) | 60.3 | 90.4 | 185.3 |
| $\rho \times 10^{-28}$ (atoms m$^{-3}$) | 9.95 | 9.95 | 8.64 |
| $A \times 10^{20}$ (J) | 5.51 | 5.69 | 7.54 |
| $C \times 10^{79}$ (Jm$^6$) | 5.64 | 5.82 | 1.03 |
| $D$ (Å) | 4.80 | 4.50 | 6.22 |
| $\lambda$ (Å) | 1.26 | 1.26 | 1.30 |
| $N_l$ | 24 | 23 | 30 |
| $L_l$ (Å) | 30.2 | 28.3 | 39.1 |
| $W_l$ (kJ mol$^{-1}$) | 3.00 | 3.91 | 1.81 |
| $l_k$ (Å) | 14 | 11 | 18 |
| $W_k$ (kJ mol$^{-1}$) | 1.37/1.18 | 1.60/1.34 | 0.84/0.72 |

**Table 2**

Flow activation energy measured by rheometer experiments of several polymers. The first three iPP are different grades of isotactic polypropylene; F1751, F1571, and F1471 are different syndiotactic grades. Information about their molecular weight and flow activation energy was obtained from reference 25. Data for PE were obtained from reference 21 and that of iPP is shown in Fig. 6.[31] Information about PS was obtained by us from results of small amplitude oscillatory shear experiments. PPMoplen is the grade Moplen HP501M from Basell and PS2 was provided by Innova S.A

| | $M_w$ (kg mol$^{-1}$) | $M_w\, M_n^{-1}$ | $E_a$ (kJ mol$^{-1}$) |
|---|---|---|---|
| iPP220 | 224.3 | 4.2 | 40.5 |
| iPP300 | 334.5 | 4.12 | 38.5 |
| iPP520 | 517.0 | 4.69 | 41.0 |
| F1751 | 88.9 | 2.8 | 50.2 |
| F1571 | 136.3 | 3.48 | 50.6 |
| F1471 | 181.3 | 3.95 | 49.3 |
| PE | 380 | 2.1 | 26.6 |
| PPMoplen | 150.8 | 6.15 | 44.6 |
| PS02 | 271 | 2.0 | 95.5 |

continuous equations, Equations (1) and (2), respectively, is around 15%. As expected, larger differences between the values evaluated with the two equations occur for interacting chain segments with low length, and they almost vanish when this length increases to 60 Å (differences below 2%). The two values become coincident for aligned chain segments of length around 10 Kuhn monomers, which is the number of statistical monomers that a chain segment must have for application of Gaussian statistics (see inset in Fig. 2).

Interactions between parallel chain segments with an energy equal to the thermal energy of the melt at 200°C would require aligned chain segments with lengths of around 60 Å for PE and 100 Å for PS. Interacting chain lengths with this value, involving segments of two chains only, violates the Maxwell–Boltzmann distribution of the relative population of different conformational states. These results indicate that entanglement effects cannot be described considering only binary interactions between two Kuhn monomers or slip-links. Higher interaction energies should be associated with entanglement interactions for explaining elastic effects in polymer melts.

Based on results of Fig. 2 and Table 1, one may anticipate that interactions of two Kuhn monomers in one chain segment with another six Kuhn monomers of different chain segments would already yield interaction energies around 10 kJ mol$^{-1}$ (for PE and iPP). However, this implies that entanglements should be viewed, then, as short-range local ordered regions containing in this case two Kuhn monomers of seven chain segments in parallel. These regions are spaced from each other by the average distance $\langle r \rangle_e = \sqrt{N_{k,e}}\, l_k$, where $N_{k,e}$ is the number of Kuhn monomers between entanglements, each with length $l_k$. The key question to accept this new view of "entanglement interactions" is the value of energy that should be ascribed to an entanglement interaction, more specifically, if the 10 kJ mol$^{-1}$ mentioned above is, or is not, a reasonable value to describe, from a physical point of view, the effects assigned to entanglements. This issue is also discussed below.



## Interaction Potential Energy between a Loop and a Chain at Its Center

Explicit expressions for evaluating the interaction potential energy between a chain and a loop, which is the best geometrical representation of a topological constraint, have not been published so far. Figure 3 shows the geometrical construction used for this evaluation. It is

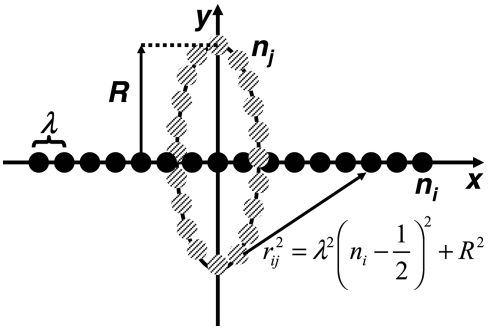


**Figure 3.** Model used to evaluate the interaction potential energy between a chain (filled circles) and a loop (dashed circles). The separation between consecutive molecules in the chain and at the loop is λ. The loop radius is $R$ and $|r_{ij}|$ is the distance between a molecule at the chain and another at the loop. The origin of the coordinate system is set at the crossing point between the loop plane and the chain axis.

considered a closed loop of $N_l$ atoms, but an open loop (or a helix turn) could also have been considered yielding a final result similar to the simpler geometrical representation of Fig. 3. The separation between two consecutive $n_j$ units is $\lambda$ and the loop radius is $R$. The loop is in the $yz$ plane. A linear chain with $N_c$ atoms (along the $x$ axis), also with a separation between two consecutive $n_i$ units of $\lambda$, crosses the center of the loop. The distance between any $n_j$ atom in the loop and any $n_i$ atom in the chain is

$$r_{ij} = \left[\lambda^2\left(n_i - \frac{1}{2}\right)^2 + R^2\right]^{1/2}. \tag{4}$$

Considering the additivity of interactions, and isotropy of the loop and chain with respect to their radius and axis, respectively, the interaction potential energy between the loop and chain is

$$W_l = -2\sum_{n_i=1}^{N_c/2}\sum_{n_j=1}^{N_l}\frac{Cn_j}{\left[\lambda^2\left(n_i - \frac{1}{2}\right)^2 + R^2\right]^3}. \tag{5}$$

The factor 2 results from the interactions at the right- and left-hand side of the loop. Equation (5) may be written as

$$W_l = -\frac{2CN_l}{\lambda^6 N_c^5}\sum_{n_i=1}^{N_c/2}\frac{1}{\left[\left(\frac{2n_i-1}{2N_c}\right)^2 + \frac{1}{\alpha^2}\right]^3}\left(\frac{1}{N_c}\right), \tag{6}$$

with $\alpha = 2\pi N_c/N_l$. The length of the loop is $L_l = 2\pi R = N_l\lambda$. Defining $y = (2n_i - 1)/2N_c$, for a long chain the above summation may be replaced by an integration with adequate changes in the integration limits,

$$W_l = -\frac{2\,C\;N_l}{\lambda^6 N_c^5}\int_{1/2N_c}^{(N_c-1)/2N_c}\frac{dy}{\left[y^2 + \alpha^{-2}\right]^3}\cdot, \tag{7}$$

whose solution, also in the limit of a very long chain, is

$$W_l \cong -\frac{3\pi C\alpha^5 N_l}{8\lambda^6 N_c^5} = -\frac{3\pi CN_l}{8\lambda R^5} = -\frac{3\pi CL_l}{8\lambda^2 R^5}. \tag{8}$$

The above equation is identical to Equation (2), the difference being in the length of the chain, which is replaced by that of the loop. It is also independent of chain length, as expected, because of the approximation made in the limit of very long chains.

Figure 4 shows the results obtained with Equations (5) and (8) for the same polymers as in Fig. 2. The interaction potential energy between the loop and a chain is plotted as a function of the chain length from the center of the loop to the left or to the right. The value on the ordinates is the interaction potential energy per mole of loops. All values indicated, with the exception of those for iPP, are below the melt thermal energy. Values for iPP obtained with Equation (8) are almost coincident with the melt thermal energy at 200°C. The interaction potential energy increases by increasing the number of chain segments and it stabilizes after five chain segments to the left and another five segments to right of the loop, all around one Kuhn monomer in length.

Because the values indicated in Fig. 4 refer to the interaction energy per mole of loops, it may be argued that since a high molecular weight chain may have several loops

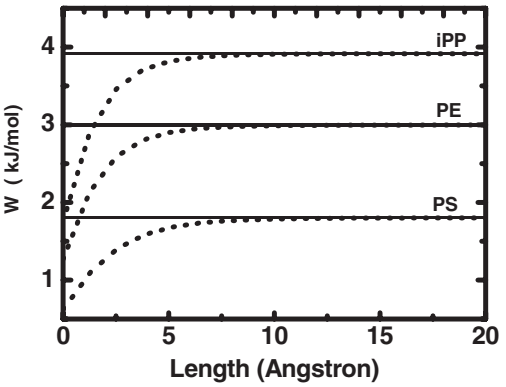


**Figure 4.** Interaction potential energy between a chain and a loop evaluated with Equations (5)—dotted line—and (8)—solid line. Due to the symmetry of the interaction between the loop and the chain with respect to the center of the loop, only values corresponding to interactions at one side of the loop (left or right) are indicated.



(entanglements) with other neighboring chains, the interaction potential energy between a loop and a chain per mole of loops in a chain has a higher value, rendering, therefore, to the chain loops a role in the flow properties of polymer melts. If this was the case, then the flow activation energy of polymer melts, evaluated in the high-temperature flow region, should consistently increase with the polymer molecular weight. As shown below, and also in other literature results,[11] this is not the case.

Results in Fig. 4 also depend on the separation distance between the chain and the loop. For their evaluation, as well as for the results in Fig. 2, use of available experimental results for the nearest intermolecular separation distance in the corresponding melt states was made. Therefore, the values shown in Fig. 4 and Table 1 represent, in principle, the highest possible values for the interaction potential energy between the chain and the loop. It results from Equations (5) and (8) that larger loop radius yield much lower, and ineffective, interaction potential energies.

## Validity of Results Obtained for the Interaction Potential Energy

Because the results indicated in the last two sections exclude binary interactions between chain segments and chain loops as a possible source of entanglements' effects, one may question the accuracy of the evaluations made for these interaction potential energies. Although the above interactions may exist between polymer chains in the molten state, the results obtained indicate that they are ineffective.

The main criticisms raised to the Salem's equation—Equation (2)—result from the procedure used in the evaluation of the London constant. Three main criticisms were raised that may be applied also to the derivation procedure of Equations (5) and (8). Two of them were due to Zwanzig[8] and the other was made by Langbein.[10] The two corrections made by Zwanzig are the pairwise additivity and the isotropy of the polarisable groups in the chain. Still, another effect, not considered by Zwanzig, was the omission of intrachain interactions.[12] However, evaluation of this additional effect lead to the equation already derived by Zwanzig, with similar numeric coefficients, and the results obtained with these corrections were not very different from those of Salem.[9,13]

The other correction, made by Langbein,[10] considered the effect of other interactions, besides the dipole–dipole interaction, on the van der Waals interaction energy. He started with the argument that an electric field of a dipole fluctuation of atom 1 at the position of atom 2 ($T_{12}$) induces a reaction field $T_{12}\alpha_2(\omega)T_{21}$ of atom 2 that lowers the energy of the original fluctuation at atom 1, where $\alpha_2(\omega)$ is the atomic polarizability. He then applied the fluctuation–dissipation theorem to obtain the van der Waals energy between atoms 1 and 2 ($W_{12}$) that was expressed as an integral over all the frequency range of the imaginary part of the Fourier transformed polarizability—Equation (2) in reference 10,

$$W_{12} = -\frac{h}{8\pi^2}\int_{-\infty}^{+\infty} d\omega \,\mathrm{tr}\left[\alpha_1(i\omega)\, T_{12}\, \alpha_2(i\omega)\, T_{21}\right]. \tag{9}$$

For dipole–dipole interactions, and assuming isotropic polarizabilities, application of this equation to two parallel cylinders, cylinders 1 and 2, with length $L$, and density of atoms $\rho_1$ and $\rho_2$, respectively, leads to

$$W = -\frac{h}{8\pi^2}\int_{-\infty}^{+\infty} d\omega\, \rho_1\alpha_1\, \rho_2\alpha_2 \int_1 \int_2 ds_1\, ds_2 \frac{9\pi L}{8\,|s_1 - s_2|^5}, \tag{10}$$

where the last two integrals are performed over the cylinder axis. Their solution was also obtained by Langbein. He found for dipole–dipole interactions a similar dependence of the interaction potential energy as in Equation (2), i.e., $W \propto L/\lambda^2 D^5$, and that the terms resulting from contributions of higher-order interactions were of order $1/D^7$ for dipole–quadropole interactions and $1/D^9$ for quadropole–quadropole interactions. The integral over the frequency for the atomic polarizability of atoms 1 and 2 may be expressed as a function of $\varepsilon(i\nu)$, the dielectric constant at the imaginary frequency $\nu$, by[5]

$$\varepsilon(i\nu) = 1 + \frac{(\varepsilon - n^2)}{(1 + \nu/\nu_{rot})} + \frac{(n^2 - 1)}{\left(1 + \nu^2/\nu_e^2\right)}, \tag{11}$$

where $\nu_{rot}$ is the molecular rotational relaxation frequency (lower than $10^{12}$ $s^{-1}$) and, as mentioned above, $\nu_e$ is the main electronic absorption frequency in UV ($\cong 2.4 \times 10^{15}$ Hz). Equation (11) is related to the total Hamaker constant[4,5]

$$A_{total} = \frac{3}{2}k_B T \sum_{n=0}^{\infty}{}' \bar{\Delta}_{1m}^2, \tag{12}$$

with $\bar{\Delta}_{1m} = [\varepsilon(i\nu_n) - \varepsilon_o]/[\varepsilon(i\nu_n) + \varepsilon_o]$. For $n \geq 1$, $\nu_n = (2\pi k_B T/h)n$. The prime in $\sum'$ indicates that the $n = 0$ term is multiplied by 1/2, yielding the zero-frequency contribution in Equation (3). The sum is over the different absorption frequencies. The zero-frequency contribution yields the term $A_{\nu=0}$ in Equation (3) and the $n \geq 1$ yield the $A_{\nu>0}$ dispersion energy contribution. Use of Equation (3a) requires knowledge on how the dielectric permittivity of the polymer changes with frequency. For some polymers this information is available.[4] We must distinguish $n$ in Equation (3a) from the material refractive index in Equations (3) and (11). Considering further that the dispersion energy is determined solely by the electronic absorption frequency in the UV, i.e., $\nu_e = \nu_1$, one obtains Equation (3) for the "symmetric case" of two phases interacting across vacuum.[5]

We thus conclude that values of the interaction potential energy evaluated with the above equations are reliable results. Their reliability may be documented further with more complicated theoretical approaches that used the density-functional theory[14] and also yielded Salem's equation in the asymptotic limit of large chain separations such that only dipole–dipole interactions are relevant, and in the absence of retardation effects due to the finite velocity of light. Experimental results also confirm the validity of the above predictions. It is considered that chain uncrossability is better demonstrated by experiments with ring polymers since only they are capable of forming mathematically rigorous topological "knots" with neighboring chains that permanently prevent chain crossing.[15] However, direct measurement of confining forces in concentrated solutions of linear and circular polymers demonstrate that the confining force imposed by circular polymers was substantially lower and of shorter range than that measured with linear polymers.[16] Based on these results, it was concluded that circular chains are less effective than linear chains at producing restrictive entanglements. Still another demonstration that the looping picture cannot explain the elastic properties of polymer melts was obtained with experiments performed with entangled ring polymers, more specifically, entangled ring polystyrenes. It was found that the relaxation modulus of entangled ring polymers does not show any plateau, and that a plateau modulus is only observed when small fractions of linear polymer chains are added to the entangled ring polymers.[17] The result of this experiment is in agreement with the results obtained above for the interaction potential energy between a loop and a chain (Fig. 4).

We conclude, therefore, that additional possible sources of intermolecular interactions need to be found for explaining this elasticity. The only remaining intermolecular interactions are those involving short-range ordered regions. However, to evaluate the dimension of these short-range ordered regions one needs to estimate the interaction potential energy responsible for the "entanglement interactions." This estimation is made below by assigning a physical meaning to the flow activation energy.



## Measurement and Physical Meaning of Flow Activation Energy

Flow activation energy may be evaluated from experiments involving different techniques, namely rheology and NMR. Most evaluations made from rheological experiments imply a simple curve shifting procedure, based on the application of the time-temperature superposition principle, and a plot of the logarithm of the shift factors against the reciprocal of the absolute temperature. Providing that the fluids in question are thermorheologically simple, time–temperature superposition can be applied. The same principle can also be applied to NMR experiments providing that all molecular processes that influence the spin-lattice relaxation time ($T_1$) obtained at different Larmor frequencies, or other NMR observables, have the same temperature dependence.[18] Depending on the temperature range studied, the temperature dependence that provides the superposition of $T_1$ (or other observable) may be fitted to a Vogel–Tamman–Fulcher, Williams–Landel–Ferry, or an Arrhenius equation.

For linear polymer chains, in the high-temperature flow region, the temperature dependence of viscosity follows the Arrhenius equation.[19–21] This experimental fact deserves careful analysis, but first we need to assign a physical meaning to flow activation energy.

A physical meaning can be assigned to any activation energy providing that the conditions for the application of reaction rate theory be fulfilled, namely, existence of microscopic reversibility and verification of the principle of detailed balance.[22–24] In rheological

experiments, flow activation energy is evaluated in the viscoelastic linear regime by application of small amplitude oscillations at a constant stress, or at a steady state. We assume, therefore, the fulfillment of the above two conditions at the scale level down to one chain segment: in the high-temperature flow region, the population of different conformational states is determined by the Boltzmann distribution and, at a specific melt temperature, changes of this population distribution by flow in the linear viscoelastic regime, or at steady state, are a dynamic process with microscopic reversibility, just like the kinetics of a reaction driven by the application of an external field.

To discriminate the different contributions to flow activation energy, as in the tube model, we select a test chain randomly from a set of linear chains in the melt. Instead of a Gaussian chain, we consider here segments in this real test chain and analyze the energy barriers found by these segments in their diffusional movement. The first obvious energy barrier to consider is the barrier height between *trans* and *gauche* conformations. Neither this, nor other, energy barriers can be considered in the Gaussian chain models since chain segments in those models are energetically undistinguishable.

One needs to find out, then, if the energy barrier for local and correlated conformational transitions matches with the value evaluated from experiments for flow activation energy. If this is the case, then flow in polymer melts proceeds exclusively by conformational transitions, chains are ideal, and no other intermolecular interactions need to be considered. Otherwise, besides this energy barrier, one needs to consider in addition other energy barriers. They may result from the chain intertwining (interaction between a loop and a chain), interactions between two Kuhn monomers of the same, or different, chains, or still from short-range local ordered regions. Other additional factors that may contribute to increase the flow activation energy, namely chain branching, ionic interactions, or chain crosslinking, are not considered in this analysis, but their contribution may be independently evaluated by performing a set of experiments with model polymer systems.

As shown in Table 2, different polymers have different values of flow activation energy.[21,25] An inspection of the results shown in this table allows concluding that flow activation energy is independent of polymer molecular weight (providing that the chain molecular weight is above the critical molecular weight),[11] and that it increases for bulkier polymer chains. This simple experimental observation induces the conclusion that the energy barriers for local and correlated conformational transitions must have a key role in the definition of flow activation energy value. Because flow activation energy is almost independent of polymer molecular weight for $M > M_c$,[11] it remains to be clarified the role played by the interchain interactions in the chain motion.

### *Does Flow in Polymer Melts Proceed Uniquely by Conformational Transitions?*

Contradictory experimental results were given by the same group of authors,[18,26,27] discussed below, concerning this specific point. Following the above discussion, an analysis is made below for the experimental values of the flow activation energy, and of energy barriers for conformational transitions, evaluated from NMR experiments for diluted solutions, unentangled, and entangled polymer melts.

The evaluation of the above energy barriers from NMR experiments is a complicated process, and it must be carefully analyzed. It implies the use of a specific model equation (or combination of models) to describe the decay with time of the $C-H$ vector orientation autocorrelation function—$G(t)$, which in polymer chains is assumed to decay to zero only when the longest relaxation time of the chain is reached.

One possible form of the orientation autocorrelation function is expressed as a linear combination of librational (*lib*), segmental (*seg*), and normal mode (*nm*) motions, each one with a specific amplitude and a relaxation function,[26]

$$G(t) = A_{lib}G_{lib}(t) + A_{seg}G_{seg}(t) + (1 - A_{lib} - A_{seg})G_{nm}(t). \tag{13}$$

Different relaxation functions were considered for each motion. Librational motion was described by a single exponential decay function with a relaxation time $\tau_{lib}$ set to a constant value of 1 ps. Most important for this discussion is the segmental relaxation function. It was described by a modified KWW equation—Equation (9) in reference 26,

$$G_{seg}(t) = \exp\{-(t/\tau_{seg})^{\beta}\}, \tag{14}$$

where $\tau_{seg}$ follows the Vogel–Tamman–Fulcher temperature dependence,

$$\tau_{seg} = \tau_{seg,\infty} \exp\{B/(T - T_0)\}. \tag{15}$$

Values used for $B$ and $T_o$ were 567 K and 212 K, respectively.

Equation (13) was substituted, in another work, by a single exponential decay function with the relaxation time expressed in the form of an Arrhenius equation—Equations (6) and (7) in reference 27,

$$G(t) = A_{seg} \exp\{-(t/\tau_{seg}) + (1 - A_{seg})\ G_{Rouse}(t)\}, \tag{16}$$

$$\tau_{seg} = \tau_{0,seg} \exp\{E_{a,seg}/RT\}, \tag{17}$$

respectively, where $G_{Rouse}(t)$ is the long-time tail part of $G(t)$.

As for the contribution of normal modes to the overall orientation autocorrelation function, it was modeled as a Rouse chain with *artificial* corrections for entanglements, in which the modes $a$ corresponding to the segments longer than the entanglement length were scaled as $a^{3.5}$ while those of lower length were scaled as $a^2$—Equations (10) and (A.6)–(A.8) of reference 26. The longest Rouse relaxation time was also expressed in the form of an Arrhenius equation with specific activation energy. All of these different approaches were used to fit the experimental $^{13}C$ NMR spin-lattice relaxation time (and also the nuclear Overhauser effect) obtained for unentangled PE solutions[27] and atactic PP melts.[18,26]

This type of analysis of NMR experimental results led authors of the same group to the following two contradictory conclusions. In references 18 and 26, where the VTF equation—Equation (14)—was used to fit the experimental data, it was found that the energy barrier for "conformational transitions" in entangled aPP polymer melts was similar to that of viscosity—around 41 kJ mol$^{-1}$.[25] This conclusion was drawn because values obtained for constants $B$ and $T_0$ were similar to those obtained for the temperature variation of viscosity. It was therefore concluded that "*rearrangement of chain conformation required for flow is simply the result of many independent conformational transitions.*" Note again that this conclusion was obtained by considering the temperature dependence of the segmental relaxation time according to a modified KWW equation,[18,26] with the temperature dependence of relaxation time given by the VTF equation. This conclusion is wrong and the reason is presented below.

Similar analysis of the NMR experimental results for low molecular weight unentangled polyethylene melts,[27] with the temperature dependence of the segmental relaxation time now following an Arrhenius equation—Equations (15) and (16), led the same group

of authors to the contradictory conclusion that "*the activation energy for conformational dynamics was 16.6 kJ/mol, significantly less than flow activation energy for linear chains of polyethylene melts,*"[27] which is around 26 kJ $mol^{-1}$ and that "*the conformational transitions are not the fundamental motions for flow in polyethylene.*"

The source of these differences was not discussed by the authors.[18,26,27] In separated works, they limited their analysis to the conclusion that flow in polypropylene melts proceeds uniquely by conformational transitions, while these same transitions are not the fundamental motions for flow in polyethylene! Although it seems acceptable that flow activation energy in unentangled, low molecular weight polymer melts, should be lower than the flow activation energy in entangled polymer melts, the physical origin of the barriers to the flow cannot be different for polyethylene and polypropylene. The source of the difference in the values of the flow activation energy of unentangled and entangled polymer melts should be ascribed only to the entanglement's effects, and not to the polymer chemical structure. Note also that flow activation energy increases with molecular weight up to a limiting value for chains with molecular weight higher than the critical molecular weight (between two and four times $M_e$).

A confirmation of the above explanation is given in the discussion below. There, experimental results are presented for local and correlated conformational transitions in diluted solutions of polypropylene with different tacticity. These results were also obtained by NMR experiments similar to those carried out by the above group of authors.[18,26,27]

A different form of the orientation autocorrelation function, probably physically more acceptable, is based on a detailed analysis of relaxation data for several polymer systems, in solution and in the bulk, well above the glass transition temperature.[28] It was verified that the $^{13}C$ spin-lattice relaxation can be described in terms of a damped diffusion of bond orientation along the chain sequence, which represents the segmental motions, and an independent fast bond librations—Equation (7) in reference 28,

$$G(t) = (1 - a) \cdot \exp(-t/\tau_2) \cdot \exp(-t/\tau_1) \cdot I_0(t/\tau_1) + a \cdot \exp(-t/\tau_0). \qquad (18)$$

where $a$ is a constant related to the half-angle of the libration cone, $I_0$ the zero-order modified Bessel function, which accounts for the damped diffusion of bond orientation, and $\tau_0$, $\tau_1$, and $\tau_2$ are the characteristic times for fast librations, for the diffusion of bond orientation along the chain and for the orientation loss process, respectively.

The relaxation time of the segmental motions ($\tau_1$) was expressed in the form of an Arrhenius equation, which allowed the evaluation of an activation energy for the relaxation of meso and racemic sequences in diluted solutions of iPP, sPP, and aPP, with molecular weight above $M_e$. Similar activation energy values (around 22 kJ $mol^{-1}$) were obtained for meso and racemic sequences. This activation energy was considered to be the height of the energy barrier for local and correlated conformational transitions in polypropylene, which is independent of tacticity. This value is much lower than the flow activation energy values of iPP, aPP, or sPP, $\approx$41 kJ $mol^{-1}$ for the first two, and $\approx$50 kJ $mol^{-1}$ for the last one—see Table II.[25,29]

From this discussion and that of the previous section, the following conclusions can be drawn:

1. The height of the energy barrier for local and correlated conformational transitions can only be evaluated in *diluted polymer solutions or in unentangled polymer melts*. The reason of this assessment, besides the difference in the experimental results mentioned above, is that for a set of segments in one chain to flow past the segments of other neighboring chains, they must first get rid of interchain interactions, and

further change their conformational states. Interchain interactions are, in principle, absent in diluted polymer solutions and in unentangled polymer melts. A proof for the last assessment is obtained from experimental results of Pearson et al.,[11] for the flow activation energy of unentangled polyethylene melts (and also for *n-alkanes*) evaluated from the temperature variation of the absolute viscosity. They indicate that the flow activation energy of unentangled PE melts at 150°C is around 18 kJ $mol^{-1}$, similar to the value of 16.6 kJ $mol^{-1}$ indicated above. In fact, what was measured by Pearson et al., for unentangled PE and *n-alkanes* was an activation energy for conformational transitions which, due to the absence of intermolecular interactions, is also a flow activation energy. Increasing the polymer molecular weight, this flow activation energy increases and, for polymers with a molecular weight higher than the critical molecular weight, the flow activation energy stabilizes at around 26 kJ $mol^{-1}$.

2. Flow activation energy measured from rheological or NMR experiments, *but in concentrated solutions or entangled polymer melts*, contains, besides the energy barrier for local and correlated conformational transitions, an additional contribution that needs to be explained. This contribution can only be a consequence of interchain interactions and it is the difference between the experimental values of flow activation energy and the experimental values for the energy barrier height of local and correlated conformational transitions. For linear polymer chains this contribution may result from the chain intertwining (interaction between a loop and a chain), which as shown above, is similar to the thermal energy of the melt, interactions between two Kuhn monomers of the same, or different, chains, or still from short-range local ordered regions.

The experimental results reported above for atactic PP melts obtained from NMR experiments[18,26] are actually flow activation energies and not, as considered by the authors, activation energies for conformational transitions. They represent activation energies for segmental motion, which proceeds by interchain interactions and conformational transitions. The flow of interacting chain segments requires energy barriers higher than those of intrachain interactions expressed by the height of the energy barrier for local and correlated conformational transitions.

### *What Are the Contributions to the Flow Activation Energy of the Interactions between a Loop and a Chain, and between Two Parallel Kuhn Monomers?*

It was shown above that the interaction between a loop and chain, which pretends to represent the chain intertwining, is too small to explain, in linear polyethylene, the increment from 16.6 kJ $mol^{-1}$ to the measured value of flow activation energy ($\approx$26 kJ $mol^{-1}$) and the different values obtained for iPP diluted solutions and entangled melts, $\approx$22 kJ $mol^{-1}$ and $\approx$41–44 kJ $mol^{-1}$, respectively—see Table 2.

In summary, one needs to explain an increment of around 10 kJ $mol^{-1}$ in PE and around 22 kJ $mol^{-1}$ in iPP. Due to the large discrepancy in the values estimated for the energy barrier height of local and correlated conformational transitions in PS, between 60 kJ $mol^{-1}$ and 112 kJ $mol^{-1}$,[30] we will not discuss further the PS results.

The maximum value for the interaction potential energy between a loop and an iPP chain is $\approx$3.9 kJ $mol^{-1}$ of loops. Still, as an academic exercise, we could consider the looping interaction as the possible source of the above difference. Then one would expect an increase in the flow activation energy by increasing the number of chain loops. Besides

the results in reference 11, experimental results shown in Table 2 contradict this assumption. For isotactic polypropylene (first and second set of rows in Table 2), flow activation energy is, within the experimental measurement errors, independent of molecular weight.

Another argument, more against the role of chain loops in the flow activation energy, is the experimental verification of different reptation time values for fully relaxed melts and for melts sheared up to a steady state—see Figs. 5 and 6. Experimental details of the results shown in these two figures may be found in reference 31. Small amplitude oscillatory shear deformations were performed in a temperature range between 180°C and 240°C in fully relaxed iPP melts and in melts sheared up to a steady state, where the melt viscosity is constant, but lower than that of fully relaxed melts, which may be evaluated by extrapolation to zero-shear-rate viscosity. These experiments allowed us to evaluate different reptation times (Fig. 6) and similar flow activation energy values (Fig. 5) for these two melt states. The reptation time was evaluated at the crossing point between $G'(\omega)$ and $G''(\omega)$ for different temperatures, in the two melt states, relaxed and the steady state in shear flow. As expected, the reptation time was lowest for melts sheared up to a steady state, indicating that around 2/3 of the entanglements existing in a fully relaxed melt were destroyed during the transition to the steady state. The measured independence of flow activation energy on the number of entanglements confirms that their number, providing that it is above a critical value, does not have any effect on the definition of values for the flow energy barrier.

These experimental results, and the discussion made in the previous section, definitely exclude chain loops as the source of melt elasticity and resistance to the flow. This does not



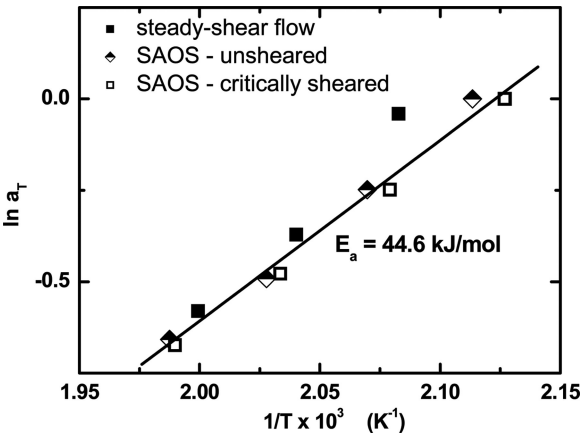


**Figure 5.** Logarithm of the shift factors as a function of the reciprocal of temperature for unsheared (filled squares) and critically sheared (half-filled lozenges) iPP melts. All evaluations were made from small amplitude oscillatory shear (SAOS) experiments, obtained in the linear viscoelastic regime. Results obtained from steady shear experiments (flow curves) are represented by squares. The solid line is a linear fit to the data. The average activation energy is indicated. The reference temperature was 200°C. Experiments with relaxed polymer melts were obtained after annealing at the melt temperature for 10 min before starting the experiment. Experiments with critically sheared melts were obtained after shearing the melt with constant shear rate of 5 $s^{-1}$ until the attainment of a steady state (viscosity constant with the shearing time), after which similar small amplitude oscillatory shear experiments were performed.

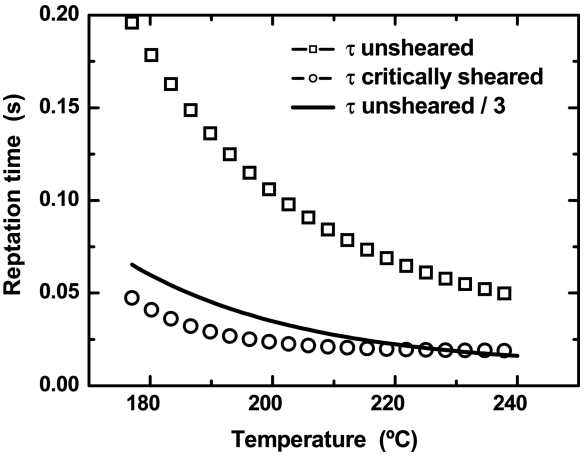


**Figure 6.** Evaluation of the reptation time from small amplitude oscillatory shear experiments for unsheared (relaxed) melts—squares—and critically sheared melts (sheared with constant shear rate up to a steady state)—circles. Represented data points are average results. Data scattering for these experiments are shown in reference 31. The reptation time was evaluated at the crossing point between $G'(\omega)$ and $G''(\omega)$. The solid line is the division by three of the reptation time values for relaxed melts.



mean that chain loops do not exist in polymer melts, but it does mean that their existence cannot explain the properties assigned to entanglements.

Because it is also considered by some authors that flow activation energy results from the monomeric friction coefficient, or better, the interaction between two parallel Kuhn monomers, this possible contribution is also analyzed. Values of this interaction energy are indicated in the last row of Table 1. They are also too small for explaining the difference between flow activation energy and the energy barriers for local and correlated conformational transitions.

It is thus demonstrated that two possible interactions that could explain the chain uncrossability, and therefore the effects assigned to entanglements, as considered for example in reference 3, the chain loops and the interaction between two Kuhn monomers in parallel, have energies below the melt thermal energy. One is led then to the obvious conclusion that short-range ordered regions have to be considered in polymer melts for explaining the above difference in activation energies, and the melt elasticity shown by different polymer systems described in the Introduction.

### *Short-Range Order in Polymer Melts*

One important problem with the existence of short-range ordered regions, or of any other type of long range correlations in polymer melts, is the validity of the "Flory theorem" on the ideality of polymer chains in melts,[32]—in a dense system of chains each chain is Gaussian and ideal—a concept that was justified further by de Gennes using a self-consistent field argument.[33] Several authors have questioned this ideality assumption with experimental, theoretical, and molecular dynamics simulation results. An example of the controversy generated by the issue of short-range order in polymer melts and in amorphous polymers in the solid state is well illustrated in volume 68 of the Faraday Discussions of Chemical Society (1979),[33–37] which may be complemented with other works by Geil in 1975[38] and

Yeh in 1980.[39] This last work provides a detailed critical review of experimental results demonstrating the existence and extent of short-range order in polymer melts. Since then, much more work demonstrating the existence of short-range order in polymer melts has been published, some of which is described below.

I will limit the presentation of experimental results demonstrating the existence of short-range order in polymer melts to a selection of works involving different materials and experimental techniques from those reported by the works mentioned in the previous paragraph. This significant amount of, so far, not contested experimental results demonstrates that now the issue does not seem any more to be the existence of short-range order in polymer melts, but rather the origin of this short-range order, how to make this short-range order consistent with the random coil model and, much more important, how the short-range order affects the flow behavior and the solidification of amorphous and semicrystalline polymers.

It is a known fact that the most basic characteristic of a low molecular weight liquid is that it possesses short-range order, and that the appropriate tool to describe this short-range order is the evaluation of the probability of finding two atoms in the liquid at a distance $r$ from each other.[40] This probability is the pair distribution function, $g(r)$, which is the inverse Fourier transform of the liquid structure factor $S(q)$. Besides this, in experiments and molecular dynamics simulations of polymers, static orientation correlations, evaluated by the orientation correlation function, are also evaluated. They indicate "*a tendency of adjacent chains to align parallel to each other at a separation distance corresponding to the intermolecular nearest neighbor packing distance,*" (see page 1131 of reference 41). In another's words "*these interchain contacts have a preference to be parallel, the two neighboring chains running along each other.*"[42]

A set of a few experimental results demonstrating the existence of short-range order in low molecular weight liquids and polymer melts is presented next. Zondervan et al., performed rheological experiments in supercooled glycerol and *ortho*-terphenyl above their glass transition temperature with a Couette shear cell by applying weak stresses.[43] They found the gradual emergence of an extended solid-like network that stiffens by increasing the aging time above $T_g$, conferring all well known features of soft glass rheology to the supercooled liquids. Among them are the gradual increase in the shear strain with time at constant stress, and the partial recovery of strain after the stress removal. The relaxation of this solid-like network persists over hours and even days, which is a clear manifestation of a memory effect, well known in other viscoelastic liquids, namely polymer melts. Zondervan et al., explained this behavior by considering that the supercooled liquid was divided into heterogeneous "liquid-pockets" separated from each other by a fragile solid-like network.

The list of recent research works in which order in melts of amorphous and semicrystalline polymers has been reported is extensive. In 1998, results of four-dimensional solid state exchange NMR experiments for poly(vinyl acetate) at $T_g + 10$ K reported heterogeneities with a dynamic length scale of $\approx$30 Å.[44] This value is considered as the upper limit for the length scale of the cooperative rearranging regions. Still in 1998, results of $^1$H double-quantum NMR experiments in poly(butadiene) melts with molecular weight above the entanglement molecular weight, suggested the existence of orientational correlations between adjacent polymer chains.[45] The quantity measured was the residual order parameter $S$ for all possible coherences (–$CH_2$, $CH_2$–$CH_2$, and CH=CH). The idea behind these experiments was that for a tagged segment its two closest entanglements serve as a constraint, impeding isotropic dynamics. Therefore, on time scales longer than the $\alpha$ relaxation time, but much shorter than the Rouse relaxation time of the chain, some residual chain order should be observed. It was found that the upper bound value for residual chain

order obtained for the influence of entanglements was $S_{C=C} \approx 0.028$, around 1 order of magnitude smaller than the experimental value, $S_{C=C} \approx 0.20$. It was concluded, therefore, that restrictions by entanglements cannot be the only source to explain the residual chain order, and that other reasons, namely orientational correlations between adjacent polymer chains, must be considered to explain the above deviation.[45]

Rheological experiments provided additional examples of order in polymer melts. Perhaps the most impressive experiment demonstrating the elasticity in polymer melts was done by Meissner in 1971.[46] Results of these experiments were reported and discussed by Lodge in 1989.[47] A stress-free sample of low-density polyethylene at 150°C was elongated at a constant rate of 1 $s^{-1}$ to a length $L_1$; the stress was removed and the sample recovered to a length $L_2$ (see Fig. 2 of reference 47). Recoveries of 10 times were observed ($L_1 = 10$ $L_2$), much larger than the maximum extensions observed in crosslinked rubbers ($\lambda \approx 7$). The following quotation is an attempt of Lodge to explain these results that led him to the formulation of the temporary-junction network model. "*In order that molecular retraction can lead to elastic recovery, we conjecture that there shall be some non-zero interaction between retracting molecules. If there are no covalent bond crosslinks, what else can there be?*" It is implicit in this reasoning the need of physical interactions between polymer molecules to explain the elastic recovery. It is clear from the results shown in the previous paragraphs that any sort of binary interactions between polymer chains cannot explain this elasticity. Other type of interactions involving a few Kuhn monomers aligned in parallel belonging to the same or different chains have to be considered.

Because elasticity in polymer melts is assigned to entanglements, it is important to mention several manifestations of elasticity and solid-like behavior in unentangled polymer melts. Two recent reports of these results were made by Collin and Martinoty (CM) in 2003,[48] and in 2006 by CM[49] and Mendil, Baroni and Noirez.[50] In these works several more references to order in polymer melts, besides those presented here, may be found. Although these two groups of authors present different explanations for their results, both concur with the idea of order in polymer melts.

The results of Mendil et al.,[50] are particularly relevant for the issue discussed here because they were performed more than 75°C above $T_g$, well within the flow region. It must be mentioned beforehand that this work was the subject of a series of commentaries by McKenna[51] and Vlassopoulos,[52] but the experimental results they reported were confirmed by other independent authors.[53] The importance of these results stems from the experimental demonstration of elasticity in unentangled polymer melts, or in the authors' own words, their solid-like rheological response. They performed nonstandard rheological experiments with unentangled polymer melts using conventional aluminum fixtures and fixtures with interacting surfaces (nearly zero contact angle with the polymer melt after 70 min of melt relaxation). An elastic response was observed when fixtures with interacting surfaces were used: $G'(\omega)$ was almost constant in the same frequency window, i.e., the unentangled melt showed a solid-like rheological response. These authors discussed, with detail, possible sources of error. They concluded that the observed elasticity is an intrinsic property of the polymer melt and that, even in the melt, the chains experience a cohesive effect of macroscopic distances.

Similar observations were made much earlier, in 1992, by Hu and Granick,[54] also for unentangled polymer melts of atactic poly(phenyl methyl siloxane) of 2240 g $mol^{-1}$ and 4620 g $mol^{-1}$ ($M_e = 12{,}000$ g $mol^{-1}$). The polymer fluid was confined between atomically smooth muscovite mica (separation distance between 60 Å and 70 Å), which has a nearly zero contact angle with the polymer melt. They studied the viscoelastic dynamics of the confined polymer melts and found that when the film diameter was less than five to six

times the unperturbed radius of gyration, a strong rubber-like elasticity emerged that was not characteristic of bulk samples. The same type of phenomena as the one reported by Mendil et al., was here observed, although in this case the result could also be ascribed to the confinement effect.

Recently, a theory of cluster formation in homopolymer melts was developed by Semenov[55] as an attempt to explain the "*many indications that some thermodynamically stable aggregates (clusters) are formed in homopolymer melts (single-component systems) in conditions far way from any phase separation.*" With this theory, it was also intended to understand the low-frequency solid-like rheological behavior of unentangled polymer melts and the elasticity of polymer melts in general. Before continuing the discussion, we insert a brief resume of this cluster formation theory.

The theory considers the formation of thermodynamically stable, finite aggregates of semicrystalline micelles in homopolymer melts providing that they are stereoisomeric. With this assumption, it is considered that even atactic polymers contain stereoregular segments that aggregate to form a lamellar crystal serving as a micelle core, surrounded by a shell of the stereoirregular parts of the chains. This model is not of universal validity since it does not explain the formation of clusters in poly(ethylene oxide) melts, and it is not clear, also, how the cluster size and number would change with the increase in the degree of stereoregularity of the polymer chains, more specifically in melts of semicrystalline polymers.

The concept of short-range ordered regions considered in this work is different from the different types of long-range correlations and cluster formation considered by the different authors quoted above. Further, because the concept of short-range ordered regions here used depends uniquely on the van der Waals interactions between chain segments, these short-range ordered regions are universal to all macromolecular materials and their number is easily estimated. It is exactly the same as that of entanglements, which means that the number of short-range ordered regions in a chain with molecular weight $M_w$ is simply $Z = M_w/M_e$, where $M_e$ is the average molecular weight between entanglements evaluated from the plateau modulus value. Their length can also be predicted, as well as their average separation distance in a fully relaxed melt. Predictions for their diameter will be presented in future works since they require more detailed explanations.

The analysis below considers only fully relaxed melts. This means that the effect of any flow deformation on the number, dimensions, and orientation with the flow direction of the short-range ordered regions is not discussed. To demonstrate the validity of the predictions for the dimensions of short-range ordered regions in polymer melts, polyethylene will be used as the model polymer. The reason for this choice stands on the experimental and molecular dynamics simulation results that indicate the existence of local correlations between neighboring chain segments for PE melts. The molecular dynamics simulation results are those indicated in page 1131 of reference 41. The experimental results are those of Fig. 2 in reference 35, as well as those presented in reference 39. There, results from WAXS experiments indicate clearly, beyond any doubts, the existence of intermolecular interactions between polymer chains. Other experimental results presented by Yeh for the differential pair correlation function in molten polyethylene indicate the existence of intermolecular correlations at 5 Å, 10 Å, 15 Å, and 20 Å.[39] These correlations indicate that short-range ordered regions in molten PE have the form of a distorted hexagonal "lattice" and that the extent of order is limited to $r = 25$ Å; in addition, values for the distortion parameters of this lattice were given. These results provide indications for the diameter of the short-range ordered regions.

A completely different procedure will be used here to evaluate the length of the short-range ordered regions in molten polyethylene. We have to explain the difference of around

10 kJ mol$^{-1}$ between the 26.6 kJ mol$^{-1}$ for the flow activation energy in entangled polymer melts (Table 2) and the 16.6 kJ mol$^{-1}$ for the energy barrier for local and correlated conformational transitions. We know from Yeh's results,[39] as well as from those of Lovel et al.,[35]] that short-range ordered regions in PE melts have hexagonal symmetry (one chain segment is surrounded by six other chain segments in similar conformational sequences) and their separation distance is around 4.8 Å. Using Equation (2), with the Hamaker constant for PE evaluated at 200°C, we find that the interaction potential energy involving one chain segment with the length of one Kuhn monomer (14 Å) interacting with the other six is 8.34 kJ mol$^{-1}$. The value of 10 kJ mol$^{-1}$ is obtained if 18 Å is considered for the length of the interacting chain segment.

The length of this ordered region, one chain segment interacting with six others, decreases by increasing the melt temperature. Since the flow activation energy in the high-temperature flow region is constant, the temperature dependence of parameters used in Equation (2) implies a decrease in length with the increase of temperature.

Predictions for the length of the short-range ordered regions are also dependent on the intermolecular separation distance and on the number of chain segments included in the ordered regions. Since we are dealing with a dynamic melt, it is reasonable to expect that the dimension and number of chains participating in these ordered regions should also have an intrinsic dynamic character. However, it is also reasonable to expect that in a fully relaxed melt their average length and the average number of chains participating in the ordered regions would be constant.

The model of melt morphology here proposed can be elaborated further by evaluating the average number of segments in one chain which are incorporated in the ordered regions and those which are in random conformational sequences. Considering the $M_w$ value of PE indicated in Table 2, and $M_e = 1500$ g mol$^{-1}$ (molecular weight between entanglements), the average number of short-range ordered regions in a chain with this molecular weight is 253. The average number of Kuhn monomers in this chain is 2533 (with $M_k = 150$ g mol$^{-1}$). Considering the value estimated above of 18 Å for the length of ordered regions, one concludes that around 325 Kuhn chain segments of one chain are incorporated in the short-range ordered regions. In other words, only 13% of the chain segments, on average, belong to the ordered regions, the remaining 87% being in random conformational sequences. Predictions with very similar final results may also be obtained for other polymers.

These results explain also the reason for the success of the random coil model in polymer melts. More than 80% of the chain segments are in random conformational sequences, and less than 20% of the chain segments are in ordered regions. Their average number is obtained by dividing the chain molecular weight by the molecular weight between entanglements. The average square distance between two consecutive ordered regions is $\langle r^2 \rangle_e = (M_e/M_k) l_k^2$, or $\langle r \rangle_e = 44$ Å. Because their interaction energy is higher than the thermal energy of the melt, they provide an explanation for the source of elasticity in polymer melts and also for the low frequency elastic behavior of nonentangled polymer melts. In fully relaxed melts these regions must have random orientation. It is reasonable to assume then, that flow deformations orientate these regions with the flow direction. Changes in their number and dimensions (diameter) with the flow direction will be discussed in future works.

In summary, the new model of the melt morphology of any fully relaxed macromolecular system, in which the macromolecules have a molecular weight higher than the critical molecular weight, considers, instead of entanglements, short-range local ordered regions, which have a length between one and two Kuhn monomers only. We understand by a fully relaxed melt, a melt in which the effects of melt memory resulting from any previous

thermal and mechanical history have been erased. Because the flow activation energy is the same for relaxed melts and melts sheared up to a steady state, the length of these short-range local ordered regions should be constant, regardless of the melt state, fully relaxed or sheared. In fully relaxed melts, the number of these short-range ordered regions is equal to that normally attributed to entanglements. The average separation distance between the ordered regions, which is evaluated using Gaussian statistics, would be equal to that of the tube diameter. The effect of shear flow on the number and diameter of short-range local ordered regions will be discussed in a future work, together with experimental results.

It is foreseen that future models for the flow behavior of polymer melts should consider a test chain confined to a tube, but the constraining of the chain should instead be described by a potential resulting from the van der Waals interactions between chain segments in the short-range local ordered regions. In this work, a method is provided to evaluate this interaction potential energy from experimental results for the flow activation energy in the high-temperature flow region and the energy barrier for local and correlated conformational transitions.



The model proposed here has some similarities to ideas proposed by Qian,[56] following a completely different approach from the one here used. He evaluated the amount of coil interpenetration as a function of the polymer molar mass from the coil and polymer melt densities, and based on results of these evaluations he concluded that "perhaps it is worthy to revisit the question of chain entanglement to determine whether it is of a topological nature or of a cohesive nature that works through local nematic interactions. At the flowing temperature of a polymer melt, the cohesive entanglements along the chain are in a state of dynamic equilibrium of entanglement and disentanglement with the neighboring chain segments of interpenetrated chains. This kind of dynamic bonding and debonding of entanglement points is a necessary condition for a van der Waals network of the polymer melt to be able to flow. ... Topological entanglements may naturally exist to a small extent, but they probably do not play a significant role in the physical properties under consideration."[56]

Since, as the result of our above explanations, elasticity in polymer melts, in general, entangled and nonentangled, was attributed to short-range ordered regions, and these regions were identified as responsible for the properties assigned to entanglements, one may question how experimental results for the observed low-frequency elasticity in polymer melts can be explained. We consider the results reported for poly(n-butyl acrylate) with $M_w = 20{,}000$ g mol$^{-1}$, $M_w/M_n = 1.1$, and $M_e = 22{,}000$ g mol$^{-1}$.[50] A low frequency elasticity was reported when small amplitude oscillatory shear experiments were performed at temperatures more than 90°C above the glass transition using alumina fixtures, instead of the standard steel or aluminum fixtures, in the rheometer. Further, as stated by the authors, the observation of this behavior required the removal of microbubles, application of long annealing and equilibration times and very small strain amplitudes. After 60 min of contact between the polymer melt and the alumina surface, the contact angle decreases to very low values. This result indicates the development of interface interactions between the plate and polymer. It is known from experiments in wetting surfaces that low conformational energy chain sequences lay longitudinally along the surface. Even in polymers with molecular weight below $M_e$ we expect the existence of one short-range ordered region, which is the result of a low energy conformational chain sequence involving one to two Kuhn monomers. Therefore, the observed elastic behavior may be explained by an orientation of chain segments of this short-range ordered region to lie flat-on in the surface (which requires some annealing time), and also of an eventual magnification in the size of this ordered region,

which implies a magnification of the interaction between polymer chain segments and the interacting surface, explaining therefore the observed low-frequency elasticity.

## Conclusions

A detailed discussion was made of the validity of the procedure used to evaluate the interaction potential energy between parallel chain segments and also between a loop and a chain at its center. It was shown that the intertwining between chains, represented with the looping picture, or any other binary interaction between chain segments, such as that involving one Kuhn monomer of each chain aligned in parallel, do not explain the properties assigned to entanglements, namely the elasticity of polymer melts. The interaction energy involved in these interactions is always below, or around, the thermal energy of the melt.

A physical meaning was assigned to the flow activation energy evaluated in the high-temperature flow region. The different possible contributions to this activation energy were discriminated. For linear polymer chains in the molten state, only two portions were considered: one contribution resulting from local and correlated conformational transitions and an additional contribution that was explained based on short-range local ordered regions.

The magnitude of this additional contribution allowed us to estimate the approximate length of these ordered regions. A detailed reference to literature supporting the existence of short-range ordered regions in polymer melts was provided and references to several works supporting the nonvalidity of the random coil model, or ideal chain behavior, were provided. It was shown that more than 80% of conformational states are in random sequences, which indicate that the random coil model is still a very good description of chain conformations in the molten state, but it is not an exact model. The nonideal behavior results from energetic interactions in the short-range ordered regions.

A new model of melt morphology, of general validity to all macromolecular systems, was proposed. This model is consistent with existing ideas of chain confinement to a tube and of its diffusional movement by reptation.



## Acknowledgments

I thank discussions with Weidong Zhang, J. J. C. Cruz-Pinto, Paulo Lopes, Zlatan Denchev, João Maia, Laurence Noirez, Jean-Pierre Ibar, and Andrzej Galeski. This work was carried out under the projects POCTI/CTM/46270/2002 and Project 3599/PPCDT-PIDDAC-PTDC/CTM/68614/2006 of the Portuguese Foundation for the Science and Technology (FCT) with funding from the POCTI and FEDER programs.

## References

1. Busse, W.F. The physical structure of elastic colloids. J. Phys. Chem. **1932**, *36*, 2862–2869.
2. Padding, J. Computer simulation of entanglements in viscoelastic polymer melts. PhD thesis, University of Twente, the Netherlands, **2002**.
3. Dealy, J.M.; Larson, R.G. Structure and rheology of molten polymers: From structure to flow behaviour and back again. Munich: Carl Hanser Verlag, **2006**.
4. Parsegian, V.A. Van der Waals forces: A handbook for biologists, chemists, engineers and physicists. New York: Cambridge University Press, **2006**.
5. Israelachvili, J. Intermolecular and surface forces. London: Academic Press Ltd. **1992**.

6. Salem, L.J. Attractive forces between long saturated chains at short distances. J. Chem. Phys. **1962**, *37*, 2100–2113.
7. de Rocco, A.G.; Hoover, W.G. On the interaction of colloidal particles. Proc. Natl. Acad. Sci. U.S. **1960**, *46*, 1057–1065.
8. Zwanzig, R. Two assumptions in the theory of attractive forces between long saturated molecules. J. Chem. Phys. **1963**, *39*, 2251–2258.
9. Margenau, H.; Kestner, N.R. Theory of intermolecular forces. Oxford, UK: Pergamon Press Ltd., **1969**.
10. Langbein, D. Van Der Waals attraction between cylinders, rods of fibers. Phys. Kondens. Materie **1972**, *15*, 61–86.
11. Pearson, D.S.; Ver Strate, G.; von Meerwall, E.; Schilling, F.C. Viscosity and self-diffusion coefficient of linear polyethylene. Macromolecules **1987**, *20*, 1133–1141.
12. Wang, S.Q.; Mahan, G.D. Normal modes and interaction energies for long chains. J. Chem. Phys. **1973**, *59*, 4029–4034.
13. Nagle, J.F.; Wilkinson, D.A. Lecithin bilayers: Density measurement and molecular interactions. Biophys. J. **1978**, *23*, 159–175.
14. Kleis, J.; Schröder, E. Van Der Waals interaction of simple, parallel polymers. J. Chem. Phys. **2005**, *122*, 164902, 1–7.
15. Zhou, Q.; Larson, R.G. Direct calculation of the tube potential confining entangled polymers. Macromolecules **2006**, *39*, 6737–6743.
16. Robertson, R.M.; Smith, D.E. Direct measurement of the confining forces imposed on a single molecule in a concentrated solution of circular polymers. Macromolecules **2007**, *40*, 8737–8741.
17. Kapnistos, M.; Lamg, M.; Vlassopoulos, D.; Pyckhout-Hintzen, W.; Richter, D.; Cho, D.; Chang, T.; Rubinstein, M. Unexpected power-law stress relaxation of entangled ring polymers. Nat. Mater. **2008**, *7*, 997–1002.
18. Moe, N.E.; Qiu, X.; Ediger, M.D. $^{13}$C NMR study of segmental dynamics of atactic polypropylene melts. Macromolecules **2000**, *33*, 2145–2152.
19. Colby, R.; Rubinstein, M. Polymer physics. N.Y.: Oxford University Press, Inc., **2003**, p. 337, eq. (8.129).
20. Donth, E. The glass transition—relaxation dynamics in liquids and disordered materials. New York: Springer, **2001**, p. 12, 14 and 15.
21. Ngai, K.L.; Plazek, D.J. Relation of internal rotational isomerism barriers to the flow activation energy of entangled polymer melts in the high-temperature Arrhenius region. J. Polym. Sci. Polym. Phys. Ed. **1985**, *23*, 2159–2180.
22. Onsager, L. Reciprocal relations in irreversible processes. I. Phys. Rev. **1931**, *37*, 405–426.
23. Pollak, E.; Talkner, P. Reaction rate theory: What it was, where is it today, and where is it going? Chaos **2005**, *15*, 26116, 1–11.
24. Henriksen, N.E.; Hansen, F.Y. Theories of molecular reaction dynamics. N.Y.: Oxford University Press, Inc., **2008**, p. 139, 304.
25. Rojo, E.; Muñoz, M.E.; Santamaria, A.; Peña, B. Correlation between conformational parameters and rheological properties of molten syndiotactic polypropylenes. Macrom. Rapid Commun. **2004**, *25*, 1314–1318.
26. Qiu, X.; Moe, N.E.; Ediger, M.D.; Fetters, L.J. Local and global dynamics of atactic polypropylene melts by multiple field 13C nuclear magnetic resonance. J. Chem. Phys. **2000**, *113*, 2918–2926.
27. Qiu, X.; Ediger, M.D. Local and global dynamics of unentangled polyethylene melts by 13C NMR. Macromolecules **2000**, *33*, 490–498.
28. Destrée, M.; Lauprête, M.F.; Lyuli, A.; Ryckaert, J.P. Local dynamics of isotactic and syndiotactic polypropylene in solution. J. Chem. Phys. **2000**, *112*, 9632–9644.
29. Pearson, D.S.; Fetters, L.J.; Younghouse, L.B.; Mays, J.W. Rheological properties of poly (1, 3-dimethyl-1-butenylene) and model atactic polypropylene. Macromolecules **1988**, *21*, 478–484.
30. Khare, R.; Paulaitis, M.E. A study of cooperative phenyl ring flip motions in glassy polystyrene by molecular simulations. Macromolecules **1995**, *28*, 4495–4504.

31. Martins, J.A., Zhang, W.; Brito, J.A. Saturation of shear-induced isothermal crystallization of polymers at the steady state and the entanglement–disentanglement transition. Macromolecules **2006**, *39*, 7626–7634.
32. Flory, P.J. The configuration of real polymer chains. J. Chem. Phys. **1949**, *17*, 303–310.
33. de Gennes, P.G. Scalling concepts in polymer physics. Ithaca, NY: Cornell University Press, **1979**.
34. Flory, P.J. Levels of order in amorphous polymers. Faraday Discuss. Chem. Soc. **1979**, *68*, 14–25.
35. Lovel, R.; Mitchell, G.R.; Windle, A.H. Wide-angle X-ray scattering study of structural parameters in non-crystalline polymers. Faraday Discuss. Chem. Soc. **1979**, *68*, 46–57.
36. Uhlman, D.R. Electron microscopy and SAXS studies of amorphous polymers. Faraday Discuss. Chem. Soc. **1979**, *68*, 87–95.
37. de Gennes, P.G. Theory of long range correlations in polymer melts. Faraday Discuss. Chem. Soc. **1979**, *68*, 96–103.
38. Geil, P.H. Morphology of amorphous polymers. Ind. Eng. Chem. Prod. Dev. **1975**, *14*, 59–71.
39. Yeh, G.S.Y. Current concepts of morphology of amorphous polymers. II. Degree of order and overall chain conformation. Polym. Sci. U.S.S.R. **1980**, *21*, 2686–2703.
40. March, N.H.; Tosi, M.P. Introduction to liquid state physics. Singapore: World Scientific Publishing Co. Pte. Ltd., **2002**, p. 75.
41. Paul, W.; Smith, G.D. Structure and dynamics of amorphous polymers: Computer simulations compared to experiment and theory. Rep. Prog. Phys. **2004**, *67*, 1117–1185.
42. Faller, R. Influence of chain stiffness on the structure and dynamics of polymers in the melt. PhD Thesis, University of Mainz, Germany, **2000**, p. 108.
43. Zondervan, R.; Kulzer, F.; Berkhout,G.C.G.; Orrit, M. Soft glassy rheology of supercooled molecular liquids. PNAS **2007**, *104*, 12628–12633.
44. Tracht, U.; Wilhelm, M.; Heuer, A.; Feng, H.; Schmidt-Rohr, K.; Spiess, H.W. Length scale of dynamic heterogeneities at the glass transition determined by multidimensional nuclear magnetic resonance. Phys. Rev. Lett. **1998**, *81*, 2727–2730.
45. Graf, R.; Heuer, A.; Spiess, H.W. Chain-order effects in polymer melts probed by $^{1}$H double-quantum NMR spectroscopy. Phys. Rev. Lett. **1998**, *80*, 5738–5741.
46. Meissner, J. Dehnungsverhalten von Polyäthylen-Schmelzen. Rheol. Acta **1971**, *10*, 230–242.
47. Lodge, A. S. Elastic recovery and polymer–polymer interactions. Rheol. Acta **1989**, *28*, 351–362.
48. Collin, D.; Martinoty, P. Dynamic macroscopic heterogeneities in a flexible linear polymer melt. Physica A **2003**, *320*, 235–248.
49. Collin, D.; Martinoty, P. Commentary on "Solid-like rheological response of non-entangled polymers in the molten state" by H. Mendil et al. Eur. Phys. J. E **2006**, *19*, 87–98.
50. Mendil, H.; Baroni, P.; Noirez, L. Solid-like rheological response of non-entangled polymers in the molten state. Eur. Phys. J. E **2006**, *19*, 77–85.
51. McKenna, G.B. Commentary on rheology of polymers in narrow gaps. Eur. Phys. J. E **2006**, *19*, 101–108.
52. Vlassopoulos, D. Commentary on the observations of solid-like rheological response in unentangled polymer melts by H. Mendil, P. Baroni, L. Noirez, D. Collin, P. Martinoty. Eur. Phys. J. E **2006**, *19*, 113–117.
53. Wang, S.Q.; Ravindranath, S.; Wang, Y.; Boukany, P. New theoretical considerations in polymer rheology: Elastic breakdown of chain entanglement network. J. Chem. Phys. **2007**, *127*, 64903, 3.
54. Hu, H.W.; Granick, S. Motions and relaxations of confined liquids. Science **1992**, *258*, 1339–1342.
55. Semenov, A.N. Theory of cluster formation in homopolymer melts. Macromolecules **2009**, *42*, 6761–6776.
56. Qian, R. A new interpretation of Mc, the critical molar mass for chain entanglement. J. Macromol. Sci. Part B **1999**, *38*, 75–77.
57. Van Krevelen, D.W. Properties of polymers, 3rd edn. Amsterdam: Elsevier Science B. V., **1997**.
58. Neelakantan, A.; Maranas, J.K. Intra- and intermolecular packing in polyolefin blends. Macromolecules **2004**, *37*, 8437–8480.

## Appendix

### A1. Temperature Variation of Van der Waals Volume

The data in Table A1 were used to evaluate the interaction potential energy between chain segments, either parallel or between a ring of segments and a chain. The van der Waals volume at room temperature ($V_{w,To}$) and molar thermal expansivity ($E_1$) were obtained from reference 57. The temperature variation of van der Waals volume was evaluated from

$$V_w(T) = V_{w,To} + E_1(T - 298). \tag{19}$$

This result was used to evaluate the number density of atoms at different temperatures, which was then included in the evaluation of London constant ($C$).

**Table A1.**
Parameters used in the evaluation of Hamaker constant and interaction energy between adjacent chain segments

| | PE | PP | PS |
|---|---|---|---|
| Van der Waals volume ($cm^3$) | 20.46 | 30.68 | 62.85 |
| Molar thermal expansivity ($cm^3$ K $mol^{-1}$) | $2.05 \times 10^{-2}$ | $3.07 \times 10^{-2}$ | $6.29 \times 10^{-2}$ |
| Dielectric permittivity | 2.30 | 2.20 | 2.55 |
| Refractive index | 1.49 | 1.50 | 1.59 |
| Number of atoms per monomer | 6 | 9 | 16 |
| Kuhn monomer diameter (Å) | 3.12 | 5.28 | 11.98 |
| Kuhn monomer molecular weight (g $mol^{-1}$) | 150 | 180 | 720 |
| Number of monomers in one Kuhn chain segment | 5.40 | 4.27 | 6.90 |



### A2. Evaluation of the Separation Distance Between Polymer Chains

Values used for the intermolecular separation distance of PE and PP melts were obtained from experimental results published in references 35 and 58. For PS, and in absence in the literature of values for the intermolecular separation distance at 200°C, this value was obtained by simulating a PS melt of two chains with molecular weight above critical molecular weight in the ChemDraw 3D software. The melt was equilibrated at 200°C for a period of 10 ns and the shortest separation distance between neighboring chain segments was evaluated. The value obtained is in Table 1.